Mon. Not. R. Astron. Soc. **000**, 1–9 (2016) Printed 17 September 2018 (MN LATEX style file v2.2)

A comparison of the $R_h = ct$ and ΛCDM cosmologies using the Cosmic Distance Duality Relation

Fulvio Melia⋆
Department of Physics, The Applied Math Program, and Department of Astronomy, The University of Arizona, AZ 85721, USA

ABSTRACT
The cosmic distance duality (CDD) relation (based on the Etherington reciprocity theorem) plays a crucial role in a wide assortment of cosmological measurements. Attempts at confirming it observationally have met with mixed results, though the general consensus appears to be that the data do support its existence in nature. A common limitation with past approaches has been their reliance on a specific cosmological model, or on measurements of the luminosity distance to Type Ia SNe, which introduces a dependence on the presumed cosmology in spite of beliefs to the contrary. Confirming that the CDD is actually realized in nature is crucial because its violation would require exotic new physics. In this paper, we study the CDD using the observed angular size of compact quasar cores and a Gaussian Process reconstruction of the HII galaxy Hubble diagram—without pre-assuming any particular background cosmology. In so doing, we confirm at a very high level of confidence that the angular-diameter and luminosity distances do indeed satisfy the CDD. We then demonstrate the potential power of this result by utilizing it in a comparative test of two competing cosmological models—the $R_h = ct$ universe and ΛCDM—and show that $R_h = ct$ is favoured by the CDD data with a likelihood $\sim 82.3\%$ compared with $\sim 17.7\%$ for the standard model.

Key words: cosmological parameters, cosmology: observations, cosmology: theory, distance scale, galaxies: active, quasars: supermassive black holes

1 INTRODUCTION

The so-called cosmic distance duality (CDD) relation, based on the reciprocity theorem first derived by Etherington (1933) (and revived by Ellis 1971), holds true as long as (i) the cosmic spacetime is based on Riemannian geometry, (ii) photons propagate along null geodesics, and (iii) the photon number is conserved. Mathematically, the CDD may be expressed in the form $\eta(z) = 1$, where

$$\eta(z) = (1+z)^2 \frac{d_A(z)}{d_L(z)} \ , \tag{1}$$

in terms of the angular-diameter distance $d_A(z)$ and luminosity distance $d_L(z)$. There are many reasons why the CDD could in principle be violated in nature, at least one of which was invoked to test non-standard cosmologies by Bassett & Kunz (2004a). The violation could arise if the spacetime is not described by a metric theory of gravity, which many believe is unlikely (see, e.g., Adler 1971; Bassett & Kunz 2004b), or perhaps because photons arriving from presumed standard candles, such as Type Ia SNe, are altered by absorption or scattering along the line of sight (see, e.g., Sikivie 1983; Bassett & Kunz 2004a; Raffelt 1999; Chen 1995; Deffayet & Uzan 2000; Khoury & Weltman 2004; Burrage 2008; Liao et al. 2015).

Following early papers on this topic by Bassett & Kunz (2004a, 2004b), many have attempted to validate the CDD using an array of observational data, typically using angular-diameter distances extracted from galaxy clusters and luminosity distances from Type Ia SNe (for a non-exhaustive list, see Uzan et al. 2004; Bernardis et al. 2006; Holanda et al. 2010, 2012; Khedekar & Chakraborti 2011; Li et al. 2011; Nair et al. 2011; Meng et al. 2012; Ellis et al. 2013; Liao et al. 2016; Ma & Corasaniti 2016; Hu & Wang 2018). The issue of some cosmology dependence in these measurements is not a trivial one, however. There is always the possibility that the assumption of a specific cosmological model biases the distances, particularly if the model is incomplete (or even wrong). Under such circumstances, tests of the CDD may not produce compelling, incontrovertible outcomes. For this reason, some (or all) violations of the CDD claimed by previous studies may simply be due to unaccounted for influences of the assumed cosmology (see, e.g., Uzan et al. 2004; Holanda et al. 2010; Li et al. 2011).

Several earlier workers have claimed to be testing the CDD in a manner that was free of any possible dependence on the cosmology, believing that the use of luminosity distances extracted from Type Ia SNe does not rely on any particular expansion scenario (see, e.g., Holanda et al. 2010, 2012; Meng et al. 2012; Liao et al. 2016). But the reality is that in order to 'turn' Type Ia SNe into standard candles, one must simultaneously optimize the unknown parameters describing their lightcurve along with the parameters of the presumed cosmological model (see, e.g., Amanullah et al. 2010). These three or four (depending on the application) so-called 'nuisance' parameters do not exist in isolation and cannot be iden-

⋆ John Woodruff Simpson Fellow. Email: fmelia@email.arizona.edu

tified properly without training the lightcurve fitter in the context of a particular cosmology to relate the lightcurves of SNe at different redshifts (for a discussion relevant to this see, e.g., Kim 2011; Yang et al. 2013; Wei et al. 2015c). It is now very well understood that Type Ia SN data reduced with ΛCDM as the background cosmology cannot be used for other models; one must of necessity re-optimize all of the parameters, including those of the lightcurve fitter, separately for each different expansion scenario.

In this paper, we attempt to test the CDD with as little dependence on cosmological models as possible, using a new approach for measuring the angular-diameter and luminosity distances. As we shall see, our method confirms the CDD at a much higher level of confidence than was achieved before. We use the measured angular size of compact quasar cores as an indicator of the angular-diameter distance, and a Gaussian Process reconstruction of the HII galaxies Hubble diagram to determine the luminosity distance. In neither case is it necessary to assume a cosmological model beforehand. As we shall see, the CDD measured in this fashion may then be used to test individual cosmologies. We introduce the data in § 2, and analyze the distance duality relation in § 3, confirming that it is satisfied at a very high level of confidence. As an example of the usefulness of this result, we then apply it to one-on-one model selection in § 4. We present our conclusion in § 5.

2 DATA

In this section, we describe two sets of data suitable for testing the CDD (derived from Etherington's reciprocity relation), one based on the angular size of compact quasar cores, from which we obtain $d_A(z)$, the other a Hubble diagram constructed with HII galaxies (HIIGx) and Giant extragalactic HII regions (GEHR) as standard candles, from which we infer $d_L(z)$. As we shall see, this test allows us to determine the redshift dependence of η without the need to pre-assume any cosmological model.

2.1 Angular size of compact quasar cores

Recent improvements in our understanding of compact quasar cores make it possible for us to identify a luminosity and spectral-index limited sample of central, opaque regions in these sources and use them as reliable measuring rods. These cores probe the geometry of the Universe over a much bigger fraction of its age (corresponding to $0 \lesssim z \lesssim 3$) than even Type Ia SNe can currently achieve. We have recently used these data to measure the redshift $z_{\rm max}$ at which the angular-diameter distance $d_A(z)$ reaches its maximum value (Melia 2018a; Melia & Yennapureddy 2018), finding that $z_{\rm max} = 1.70 \pm 0.20$—a unique new measure of the cosmic expansion (see also Cao et al. 2017). The location of this turning point is a strong function of the underlying cosmology and may be used for model selection, whose results thus far have strongly favoured the $R_{\rm h} = ct$ universe (Melia 2007; 2013b, 2016a, 2017a; Melia & Abdelqader 2009; Melia & Shevchuk 2012), followed by *Planck* ΛCDM (Planck Collaboration 2016). Several other models, including (and especially) Milne (see, e.g., Vishwakarma 2013; Chashchina & Silagadze 2015), Einstein-de Sitter (see, e.g., Vauclair et al. 2003; Blanchard 2006) and Static tired light (see, e.g., La Violette 2012) have been strongly rejected.

Given the history with the use of quasars and radio galaxies to probe the cosmological expansion, one should view the use of compact quasar cores to measure angular-diameter distance with some caution. In this paper, we demonstrate how the CDD may be tested using data such as these without the need to adopt any particular cosmological model. Nevertheless, this analysis is strongly dependent on astrophysical processes, such as the radio emission from quasar cores, that may not be completely free of unknown systematics. We must therefore emphasize that when we refer to the method employed here as being "model-independent," this designation refers solely to the cosmological background, not necessarily the physics of self-absorbed synchrotron emission in quasars and the HII line emission we shall discuss shortly.

Based on what we now know about these jet sources, we understand that their base emission is dominated by self-absorbed synchrotron radiation (Blandford & Königl 1979; Melia & Königl 1989; Melia et al. 1992; Nayakshin & Melia 1998; Liu & Melia 2001; Bélanger et al. 2004; Chan et al. 2009; Crocker et al. 2011; Trap et al. 2011), creating optically-thick structures with angular sizes in the milliarcsecond (mas) range. Their corresponding physical length (~10 parsecs) is much smaller than the large-scale environment of the host galaxies. In addition, their morphology and kinematics are regulated by just a handful of parameters linked to the central engine (e.g., the mass and spin), and typically last only tens of years (Gurvits, Kellermann & Frey 1999). One may therefore reasonably assume that the structure and size of compact quasar cores are independent of any long-term evolutionary effects in the hosts themselves (Kellermann 1993; Jackson 2004, 2008). But though the idea of using compact radio sources for the optimization of cosmological parameters was proposed almost 3 decades ago (see, e.g., Kellermann 1993), a persistent complication has been that they comprise a mixture of quasars, OVVs and BL Lacs, among several others, making it difficult to disentangle systematic differences among them from real cosmological variations.

This limitation notwithstanding, several significant improvements in selecting an appropriate sub-sample of these sources have produced a catalog suitable for use as standard rulers. The first was a constraint on their spectral index α (Gurvits, Kellermann Frey 1999), which led to the reduced sample assembled by Jackson & Jannetta (2006), which itself was extracted from an old 2.29 GHz VLBI survey of Preston et al. (1985), with additions by Gurvits (1994) (see also Jackson & Dodgson 1997). More recently, Cao et al. (2017) followed the lead established earlier by Gurvits, Kellermann & Frey (1999) and Vishwakarma (2001) in analyzing a possible mitigation of the scatter in core size by not only restricting their spectral index, but also their luminosity L. These authors showed that adopting the parametrization $\ell_{\rm core} = \ell_0\, L^\gamma (1+z)^n$, for the core size $\ell_{\rm core}$ in terms of a scaling constant ℓ_0, one could attain a remarkably uniform sample with $\gamma \approx 10^{-4}$ and $|n| \approx 10^{-3}$, by simply choosing only intermediate-luminosity radio quasars in the range $10^{27}\,{\rm W/Hz} < L < 10^{28}\,{\rm W/Hz}$ with spectral index $-0.38 < \alpha < 0.18$.

Figure 1 shows the data used in this paper, following the selection procedure described above. These are drawn from the original 613 sources of Jackson & Jannetta (2006)[1]. Using the *Planck* optimized parameters (Planck Collaboration 2016) to estimate $d_L(z)$, the flux density at 2.29 GHz yields the luminosity L, from which we extract the sub-sample with intermediate luminosities. Note that this step merely estimates L for the purpose of source selection. The *Planck* parameters are not used in any other way, so the results do not depend on the parametrization in ΛCDM. A subsequent restriction of the spectral index α generates the final catalog

[1] The full sample is also available at http://nrl.northumbria.ac.uk/13109/

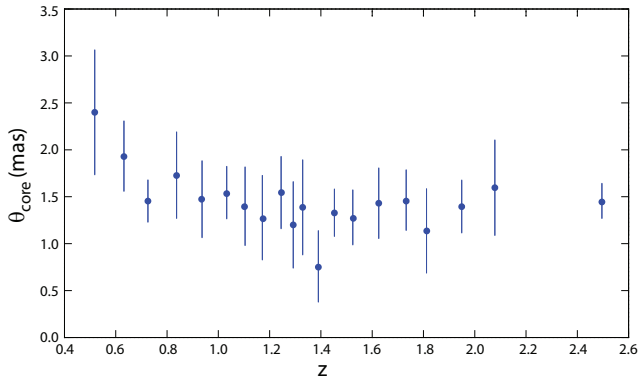

Figure 1. Angular size of 140 compact quasar cores divided into bins of 7, as a function of redshift. Each datum represents the median value in its bin, and its standard deviation is estimated assuming Gaussian variation within each bin. (Adapted from Melia 2018a)

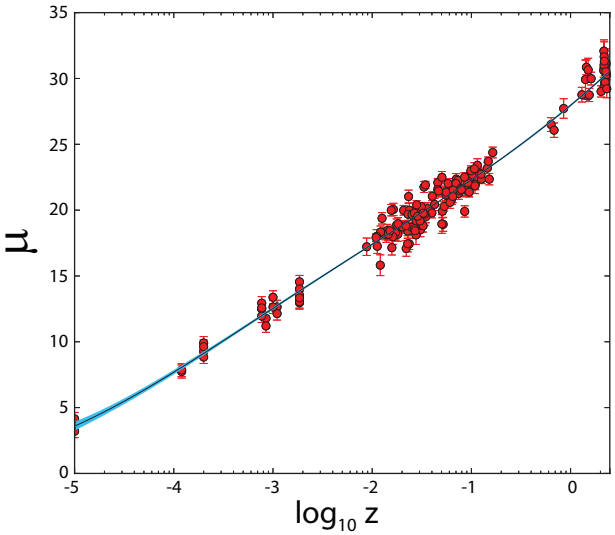

Figure 2. Distance modulus of the 156 currently available HII-region/Galaxy measurements, shown as red circles with 1σ error bars. The GP reconstructed distance modulus $\mu^{\rm obs}(z)$ is shown as a thin black curve (see text), and the blue swath represents the 1σ confidence region of the reconstruction. (Adapted from Yennapureddy & Melia 2017)

of 140 sources used in this paper. These sources are then binned into groups of 7, and the median value is chosen in each bin to represent the core angular size $\theta_{\rm core}(z)$ (Santos & Lima 2008), with associated 1σ errors estimated assuming Gaussian scatter within each bin. This step partially minimizes the scatter that would otherwise appear with individual data points, but note that it does not at all reduce the measurement uncertainty, here represented by the standard deviation σ. In other words, the remaining scatter in the individual data points is reflected in the size of the error bars associated with the 20 data points in this figure.

Writing the angular size of a compact quasar core as

$$\theta_{\rm core}(z) = \frac{\ell_{\rm core}}{d_A(z)} \ , \tag{2}$$

where $d_A(z)$ is the aforementioned angular-diameter distance, we see that, as long as the physical core size $\ell_{\rm core}$ is approximately constant in the reduced quasar sample, the measured $\theta_{\rm core}(z)$ is a valid (inverse) representation of the redshift-dependent angular-diameter distance, independent of any cosmological model. We shall describe shortly how to use the CDD in a way that avoids the need to know the actual value of $\ell_{\rm core}$.

2.2 HII Galaxy Hubble diagram

HII galaxies (HIIGx) and Giant extragalactic HII regions (GEHR) have similar optical spectra and massive star formation (Melnick et al. 1987) and their hydrogen gas, ionized by massive star clusters, emits prominent Balmer lines in Hα and Hβ (Searle & Sargent 1972; Bergeron 1977; Terlevich & Melnick 1981; Kunth & Östlin 2000). The luminosity L(Hβ) in Hβ in these structures is strongly correlated with the velocity dispersion σ_v of the ionized gas (Terlevich & Melnick 1981), apparently because both the intensity of ionizing radiation and σ_v increase with the starburst mass (Melnick et al. 2000; Siegel et al. 2005). Not surprisingly, the relatively small dispersion in the relationship between L(Hβ) and σ_v allows these galaxies and HII regions to be used as standard candles (Melnick et al. 1987, 1988; Fuentes et al. 2000; Bosch et al. 2002; Telles 2003; Siegel et al. 2005; Bordalo & Telles 2011; Plionis et al. 2011; Mania & Ratra 2012; Chavez et al. 2012, 2014; Terlevich et al. 2015; Wei et al. 2016).

All these previous applications of the L(Hβ) - σ_v correlation, however, were based on parametric fits linked to specific cosmological models. Were we to repeat this procedure here for the calculation of the luminosity distance, $d_L(z)$, our results would similarly depend on a particular expansion scenario. Instead, we follow the approach introduced by Yennapureddy & Melia (2017), in which the function representing the HIIGx and GEHR data is reconstructed using Gaussian Processes (GP)—without the preassumption of any particular cosmology (Seikel et al. 2012). With this novel statistical method, one may reconstruct the function that best fits the data without assuming any parametric form at all.

For this paper, we use the 25 high-z HII galaxies, 107 local HII galaxies, and 24 giant extra galactic HII regions (compromising 156 sources in all) from Terlevich et al. (2015). Their luminosity versus velocity dispersion correlation may be written (Chavez et al. 2012, 2014; Terlevich et al. 2015)

$$\log L(\mathrm{H}\beta) = \alpha \log \sigma_v(\mathrm{H}\beta) + \kappa \ , \tag{3}$$

where α and κ are constants. When fitting these data using a particular cosmology, one must optimize these parameters simultaneously with those of the model, but previous work has shown that they are quite insensitive to the background cosmology (Wei et al. 2016). Combining κ and H_0 together according to

$$\delta = -2.5\kappa - 5\log H_0 + 125.2 \ , \tag{4}$$

this earlier analysis demonstrated that α and δ deviate from one model to the next by only a tiny fraction of their standard deviation. For example, one gets $\alpha = 4.86^{+0.08}_{-0.07}$ and $\delta = 32.38^{+0.29}_{-0.29}$ when using the $R_{\rm h} = ct$ cosmology, compared with $\alpha = 4.89^{+0.09}_{-0.09}$ and $\delta = 32.49^{+0.35}_{-0.35}$ for ΛCDM. As noted, such small differences are well within the measurement error so, following our goal of reconstructing the correlation function independently of any model, we shall simply adopt the average values reported by Wei et al.

(2016) for these 'nuisance' parameters, which are $\alpha = 4.87^{+0.11}_{-0.08}$ and $\delta = 32.42^{+0.42}_{-0.33}$.

The distance modulus for an HII galaxy is then given as

$$\mu^{\rm obs} = -\delta + 2.5[\alpha \log \sigma_v({\rm H}\beta) - \log F({\rm H}\beta)] \,, \tag{5}$$

and since

$$\mu^{\rm obs}(z) = 5 \log \left[\frac{d_L^{\rm obs}(z)}{\rm Mpc} \right] + 25 \,, \tag{6}$$

we may write

$$d_L^{\rm obs}(z) = {\rm const.}\ 10^{\mu^{\rm obs}(z)/5} \,. \tag{7}$$

The distance moduli for the 156 sources used in this study are plotted in fig. 2, along with the GP reconstruction of the function representing them.

A full description of the GP method, as applied to sources such as the HIIGx and GEHR catalogs, appears in Yennapureddy & Melia (2017, 2018a), based on the pioneering work of Seikel et al. (2012), and we refer the reader to these publications for all the details. An important feature of the GP approach, of particular relevance to the analysis in this paper, concerns the estimation of the 1σ confidence region associated with the reconstructed $\mu^{\rm obs}(z)$ function, which is shown as a blue swath in fig. 2. The width of this region depends on both the actual errors of individual data points and on the strength of the correlation function used in the reconstruction (see, e.g., Seikel et al. 2012). The dispersion at any redshift is less than the measured standard deviation at that point when there is a large correlation in the reconstruction which, as it turns out, is the situation we have here (Yennapureddy & Melia 2017). The GP estimated 1σ confidence region is therefore smaller than the errors in the original data. This feature is one of the main benefits of using the GP approach to reconstruct the $L({\rm H}\beta)$ - σ_v correlation for this work.

There is, however, an important caveat to keep in mind with the use of these HII galaxy data and their GP reconstruction, having to do with possible unknown systematics with the HII galaxy probe. The $L({\rm H}\beta)$-σ correlation is still not completely understood. There exist uncertainties in the size of the starburst, its age, the oxygen abundance in HII galaxies and also an internal extinction correction (Chávez et al. 2016). The scatter found with the use of Equation (3) points to a possible dependence on a second parameter. In their attempt to mitigate these uncertainties, Chávez et al. (2014) found that the size of the star-forming region can serve as this second parameter. We should also keep in mind that the $L({\rm H}\beta)$-σ relation we are using ignores any rotating support for the system (as opposed to purely kinematic support). Chávez et al. (2014, 2016) have proposed using an upper limit to the velocity dispersion in order to minimize this possible effect, but then the the catalogue of suitable sources would be greatly reduced. In addition, there is no guarantee that this systematic effect would be completely eliminated. We therefore caution that, although we are not pre-assuming any particular cosmological model for this analysis, the results we present in this paper are nonetheless subject to these possible weaknesses in our derivation of the distance modulus. The hope is that future improvements in our understanding of these systems will render the HII Hubble diagram an even more robust probe of the integrated distance measure than it is now.

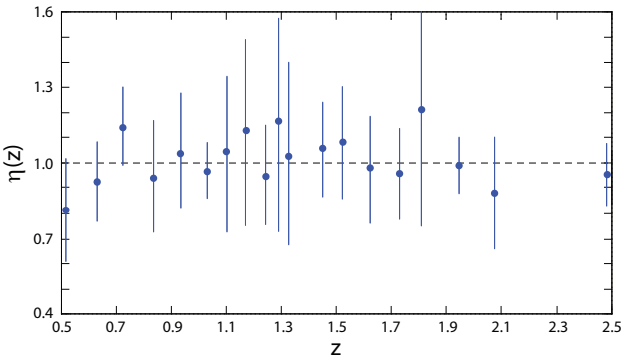

Figure 3. Values of η estimated for the 20 measured quasar core angular sizes shown in fig. 1 and the GP reconstructed Hubble diagram in fig. 2. The horizontal dashed line (i.e., $\eta = 1$) shows the value of η for a perfectly satisfied CDD. These data confirm the CDD at a very high level of confidence.

3 THE COSMIC DISTANCE DUALITY RELATION

We now have at our disposal 20 measurements of $d_A(z)$ based on the angular size of compact quasar cores, ranging in redshift from $z = 0$ to $z \sim 2.6$, and a GP reconstruction of the luminosity distance $d_L^{\rm obs}(z)$ from the HIIGx/GEHR Hubble diagram. Using our definition of $\eta(z)$ in the CDD (Eq. 1), we may assemble these data and write

$$\eta^{\rm obs}(z) = {\rm const.}\ \theta_{\rm core}^{-1}(z)\, 10^{-\mu^{\rm obs}(z)/5} (1+z)^2 \,. \tag{8}$$

The constant in this expression includes the unknown physical scale $\ell_{\rm core}$. Until this quantity is measured reliably, we are restricted in how well we can determine the absolute scaling $\eta^{\rm obs}(0)$. Nonetheless, we may use these data to measure the redshift dependence of the CDD without reference to any specific cosmological model. For this purpose, we write

$$\eta^{\rm obs}(z) = a + bz \,, \tag{9}$$

and optimize the value of the constant b using χ^2 minimization with the data shown in fig. 3. Given that we wish to avoid having to use an actual measurement of $\ell_{\rm core}$, we normalize the proportionality constant in Equation (8) to yield $a = 1$. The 20 data points plotted in fig. 3 correspond to this value of a. The associated errors are estimated using conventional error propagation,

$$\sigma_\eta = \eta^{\rm obs} \left[\left(\frac{\sigma_{d_A^{\rm obs}}}{d_A^{\rm obs}} \right)^2 + \left(\frac{\sigma_{d_L^{\rm obs}}}{d_L^{\rm obs}} \right)^2 \right]^{1/2} \,, \tag{10}$$

where $\sigma_{d_A^{\rm obs}}$ and $\sigma_{d_L^{\rm obs}}$ are the errors in $d_A^{\rm obs}$ and $d_L^{\rm obs}$, respectively, and we have assumed no covariance between these two measures of distance, given that they are based on two entirely different sets of data and analyses.

As summarized in fig. 4, our χ^2 minimization yields the following result for the fit using Equation (9):

$$\begin{aligned} a &= 1.00 \pm 0.05 \\ b &= -0.01 \pm 0.03 \,. \end{aligned} \tag{11}$$

In other words, the data shown in fig. 3 are entirely consistent with no redshift evolution at all in $\eta^{\rm obs}$, confirming at a very high level of confidence that b should be zero, as expected from the CDD. We should also point out that this test of the CDD spans an unusually large redshift range, all the way out to $z \sim 2.5$, which was not possible using solely Type Ia SN and cluster data.

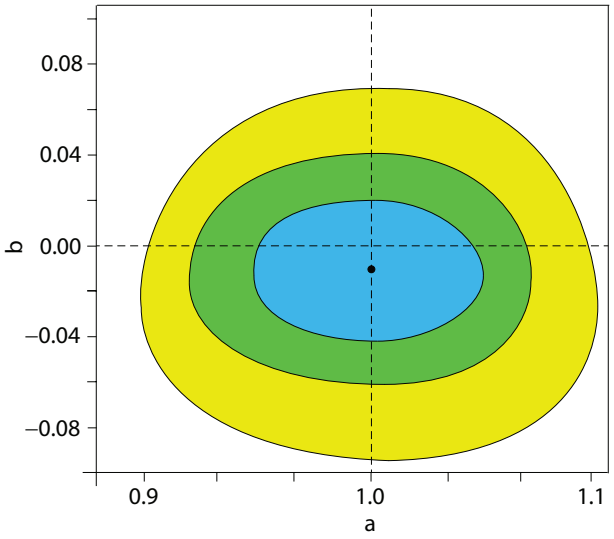

Figure 4. One (blue), two (green), and three (yellow) σ confidence regions associated with the optimized parameter $b = -0.01$ and chosen value $a = 1$ in Equation (9).

4 USING THE CDD TO COMPARE $R_{\rm H} = CT$ WITH ΛCDM

Let us now consider a simple application of this result to model selection and use the CDD data to test the $R_{\rm h} = ct$ and ΛCDM cosmologies. Of course, the angular size measurements shown in fig. 1, from which the angular-diameter distances are derived, are independent of any particular cosmological model. The optimization of cosmological parameters must therefore be carried out by finding the best fit to the luminosity distance that best accounts for the CDD in Equations (9) and (11). This presents us with a choice of either simultaneously fitting the HIIGx and GEHR Hubble diagram and the CDD, or making the model selection less dependent on data (such as HIIGx and GEHR) and simply identifying the parameters that best account for Equations (9) and (11). We should point out that our previous analysis of the HIIGx and GEHR Hubble diagram (Wei et al. 2016) already demonstrated a strong preference for $R_{\rm h} = ct$ over ΛCDM, so were we to include both the HII and CDD data in our fits, we would see an *a priori* bias towards $R_{\rm h} = ct$, in spite of the impact introduced by the CDD relation. For this paper, we therefore take a streamlined approach and simply optimize the model parameters based on the CDD data shown in fig. 3 on their own.

For the standard model, we assume a spatially flat cosmology with cosmological constant Λ. As such, the luminosity distance in ΛCDM is given as

$$d_L^{\Lambda\rm CDM}(z) = \frac{c}{H_0}(1+z)\int_0^z \frac{dz}{\sqrt{\Omega_{\rm m}(1+z)^3+\Omega_\Lambda}}\,, \qquad (12)$$

in which we have assumed a negligible radiation energy density in the local Universe. Also, $\Omega_{\rm m} \equiv \rho_{\rm m}/\rho_c$ is today's matter density in terms of the critical density $\rho_c \equiv 3c^2H_0^2/8\pi G$ and Hubble constant H_0, and $\Omega_\Lambda = 1 - \Omega_{\rm m}$. The luminosity distance in the $R_{\rm h} = ct$ universe (Melia 2003, 2007, 2013a, 2016a, 2017a; Melia & Abdelqader 2009; Melia & Shevchuk 2012) is given by the much simpler expression

$$d_L^{R_{\rm h}=ct}(z) = \frac{c}{H_0}(1+z)\ln(1+z)\,. \qquad (13)$$

Table 1. Model Selection based on the CDD

Model	$\Omega_{\rm m}$	η_0	BIC	Likelihood
$R_{\rm h} = ct$	—	0.51 ± 0.03	3.0	82.3%
ΛCDM	$0.30^{+0.26}_{-0.07}$	0.52 ± 0.03	6.0	17.7%

As was the case in Equation (8), we do not yet have an absolute measure of the core size $\ell_{\rm core}$. In writing an expression for $\eta^{\rm th}(z)$, however, one cannot optimize $\ell_{\rm core}$ and H_0 separately, and we therefore put

$$\eta^{\rm th}(z) = \eta_0\,\frac{c\,\theta_{\rm core}^{-1}(z)}{H_0\,d_L^{\rm th}(z)}(1+z)^2\,, \qquad (14)$$

where $\eta^{\rm th}(z)$ represents the CDD for either ΛCDM or $R_{\rm h} = ct$, in terms of the corresponding luminosity distance $d_L^{\Lambda\rm CDM}(z)$ or $d_L^{R_{\rm h}=ct}(z)$, and the quantity η_0 in this expression subsumes the constants $\ell_{\rm core}$, H_0 and c. Finding a best fit for ΛCDM therefore means optimizing the free parameters $\Omega_{\rm m}$ and η_0 to minimize the χ^2 function

$$\chi^2 \equiv \sum_{i=1}^{20}\frac{\left(a+bz_i-\eta^{\rm th}(z_i)\right)^2}{\sigma_\eta(z_i)^2}\,, \qquad (15)$$

where z_i are the individual redshift values in fig. 3, and $\sigma_\eta(z_i)$ is the GP standard deviation calculated in Equation (10). The analogous situation with $R_{\rm h} = ct$ requires an optimization of the sole parameter η_0.

A selection tool commonly used to differentiate between competing models (see, e.g., Melia & Maier 2013, and references cited therein) is the Bayes Information Criterion, BIC $\equiv \chi^2 + k(\ln n)$, where n is the number of data points and k is the number of free parameters (Schwarz 1978). For comprehensive model selection, one would probably use the full Bayesian evidence, rather than the BIC approximation, but this is not really necessary here, since we are merely providing a demonstration of how $\eta(z)$ may be used for this purpose. This is why we are allowing ΛCDM to have only one free parameter ($\Omega_{\rm m}$), and assuming flatness and a cosmological constant. Given the robustness of the results shown in Table 1 below, it is very unlikely that the percentage likelihoods would be reversed, or even changed significantly, with the more in-depth analysis. When $n \gg k$, as we have here, the BIC approximates the computation of the (logarithm of the) 'Bayes factor' for deciding between models (Schwarz 1978; Kass & Raftery 1995). In this limit, the posterior distribution typically becomes increasingly peaked, and Gaussian in shape. As long as one may assume that the parameters have a distribution that is unimodal and roughly Gaussian, the Bayes factor between two competing models can be calculated to high accuracy from the quotient of their respective (maximized) likelihoods. Using Laplace's method to approximate definite integrals of increasingly peaked integrands, the Kass & Raftery argument is similar to Stirling's approach of calculating an asymptotic approximation to $n!$ when $n >> 1$, given by his famous formula.

With $\rm BIC_\alpha$ characterizing model $\mathcal{M}_\alpha$, the unnormalized confidence that this model is true is the Bayes weight $\exp(-\rm BIC_\alpha/2)$.

Table 2. Model Comparisons between $R_h = ct$ and ΛCDM

Test or Observational Conflict/Tension	Outcome	Reference
Angular correlation function of the CMB	$R_h = ct$ fits it very well; standard inflationary ΛCDM misses by >> 3σ	Melia & López-Corredoira (2018)
Massive halo growth at $4 \lesssim z \lesssim 10$	Data consistent with $R_h = ct$; ΛCDM misses by $\sim 10^4$	Steinhardt et al. (2016) Yennapureddy & Melia (2018b)
Electroweak Horizon Problem	$R_h = ct$ does not have it; ΛCDM has no solution	Melia (2018b)
Missing progenitors of high-z quasars	In tension with ΛCDM, but consistent with timeline in $R_h = ct$	Fatuzzo & Melia (2017)
Angular-diameter distance test with quasar cores	$R_h = ct$ is favoured over ΛCDM with BIC likelihood 81% vs 19%	Melia (2018a); Melia & Yennapureddy (2018)
HII Hubble diagram	$R_h = ct$ is favoured over ΛCDM with BIC likelihood 93% vs. 7%	Wei et al. (2016) Leaf & Melia (2018b)
Alcock-Paczyński test with the BAO scale	$R_h = ct$ is favoured over ΛCDM at a 2.6σ c.l.	Melia & López-Corredoira (2017)
FSRQ γ-ray luminosity function	$R_h = ct$ is very strongly favoured over ΛCDM with $\Delta \gg 10$	Zeng et al. (2016)
QSO Hubble diagram + Alcock-Paczyński	$R_h = ct$ is about 4 times more likely than ΛCDM to be correct	López-Corredoira et al. (2016)
Constancy of the cluster gas mass fraction	$R_h = ct$ is favoured over ΛCDM with BIC likelihood 95% vs 5%	Melia (2016b)
Cosmic Chronometers	$R_h = ct$ is favoured over ΛCDM with BIC likelihood 95% vs 5%	Melia & Maier (2013); Melia & McClintock (2015a)
Cosmic age of old clusters	ΛCDM can't accommodate high-z clusters, but $R_h = ct$ can	Yu & Wang (2014)
High-z quasars	Evolution timeline fits within $R_h = ct$, but not ΛCDM	Melia (2013b,2018c); Melia & McClintock (2015b)
The AGN Hubble diagram	$R_h = ct$ is favoured over ΛCDM with BIC likelihood 96% vs 4%	Melia (2015)
Age vs. redshift of old passive galaxies	$R_h = ct$ favoured over ΛCDM with BIC likelihood 80% vs 20%	Wei et al. (2015a)
Type Ic superluminous supernovae	$R_h = ct$ is favoured over ΛCDM with BIC likelihood 80% vs 20%	Wei et al. (2015b)
The SNLS Type Ia SNe	$R_h = ct$ is favoured over ΛCDM with BIC likelihood 90% vs 10%	Wei et al. (2015c)
Angular size of galaxy clusters	$R_h = ct$ is favoured over ΛCDM with BIC likelihood 86% vs 14%	Wei et al. (2015d)
Strong gravitational lensing galaxies	Both models fit the data very well due to the bulge-halo 'conspiracy'	Melia et al. (2015) Leaf & Melia (2018a)
Time delay lenses	$R_h = ct$ is favoured over ΛCDM with BIC likelihood 80% vs 20%	Wei et al. (2014a)
High-z galaxies	Evolution timeline fits within $R_h = ct$, but not ΛCDM	Melia (2014a)
GRBs + star formation rate	$R_h = ct$ is favoured over ΛCDM with AIC likelihood 70% vs 30%	Wei et al. (2014b)
High-z quasar Hubble diagram	$R_h = ct$ is favoured over ΛCDM with BIC likelihood 85% vs 15%	Melia (2014b)
GRB Hubble diagram	$R_h = ct$ is favoured over ΛCDM with BIC likelihood 96% vs 4%	Wei et al. (2013)

Thus, model $\mathcal{M}_\alpha$ has likelihood

$$P(\mathcal{M}_\alpha) = \frac{\exp(-\mathrm{BIC}_\alpha/2)}{\exp(-\mathrm{BIC}_1/2) + \exp(-\mathrm{BIC}_2/2)} \tag{16}$$

of being the correct choice when dealing with a one-on-one comparison. Another way to think of this is in terms of the difference $\Delta\mathrm{BIC} \equiv \mathrm{BIC}_2 - \mathrm{BIC}_1$, which represents the extent to which $\mathcal{M}_1$ is favored over $\mathcal{M}_2$. The outcome $\Delta \equiv \mathrm{BIC}_1 - \mathrm{BIC}_2$ is judged 'positive' in the range $\Delta = 2-6$, 'strong' for $\Delta = 6-10$, and 'very strong' for $\Delta > 10$.

Our model comparison is summarized in Table 1, which displays several promising features. First, the optimization of η_0 appears to be essentially independent of the model, which suggests that both $R_h = ct$ and ΛCDM provide adequate fits to the CDD in Equations (9) and (11). Second, the optimized matter density $\Omega_m = 0.30^{+0.26}_{-0.07}$ in ΛCDM is remarkably consistent with the value $\Omega_m = 0.308 \pm 0.012$ measured by *Planck* (Planck Collaboration 2016). All of this represents an internal self-consistency that reinforces the validity of the CDD in Equations (1), (9) and (11), particularly with regard to our approach in this paper of using the quasar compact cores to measure $d_A(z)$ and the reconstruction of the HIIGx and GEHR Hubble diagram using Gaussian Processes to measure $d_L(z)$.

Nonetheless, a notable difference does emerge between these two models, directly attributable to the number of free parameters k. Once H_0 is subsumed into η_0, $R_h = ct$ has no additional degrees of freedom to use in fitting the $\eta^{\mathrm{obs}}(z)$ data in fig. 3. This is quite constraining compared to ΛCDM, in which one may adjust Ω_m to improve the fit. This added flexibility is reflected in the standard model's larger BIC, a consequence of the greater penalty imposed by the information criterion on the less parsimonious models. The magnitude of the difference $\Delta\mathrm{BIC} = 3.0$ indicates that the evidence in favour of $R_h = ct$ is positive. As a result, the likelihood of $R_h = ct$ being the correct cosmology, based on the CDD relation, is $\sim 82.3\%$ compared with only $\sim 17.7\%$ for ΛCDM.

Given this outcome, it may be helpful to compare this prioritization with the results of other comparative tests that have been reported in the literature over the past decade (see Table 2). As one may see from this list, the fact that the CDD relation tends to favour $R_h = ct$ over ΛCDM affirms the general trend seen earlier with measurements taken at both low and high redshifts, using a broad range of sources and signatures, including integrated distances and times, and also the differential expansion rate. Perhaps the most notable example of this comparison has to do with the temperature and electroweak horizon problems that require fixes to make ΛCDM work properly in the early Universe. Inflation may solve the former, but there is currently no established resolution of the latter (Melia 2018b). On the other hand, $R_h = ct$ has neither, be-

cause it avoids the early deceleration present in the standard model that produces these excessively small horizons in the first place.

Of course, there is still much to be done before one can claim that $R_h = ct$ is the correct model instead of ΛCDM. In this picture, dark energy is dynamic, not a cosmological constant, so new physics beyond the standard model of particle physics is required. It will also be essential to understand how fluctuations are produced in this cosmology, and whether they grow to properly account for the large-scale structure we see today. These are just a few of the many remaining issues that must be resolved going forward. The test reported in this paper helps to remove at least some of the uncertainty with the underlying physics, in this case having to do with the distance duality relation, which continues to build the evidence in favour of one model over the other.

5 CONCLUSION

The approach we have introduced in this paper to test the CDD appears to be an improvement over previous methods for several reasons. Once a suitable sample of compact quasar cores is selected, the use of these sources as standard rulers is rather clean—not fraught with issues, such as a complex interior structure in galaxy clusters that produces irreducible scatter in the measurement of an angular diameter distance. For example, consider the disparity produced by the comparison of two different cluster samples in Holanda et al. (2010, 2012), who reached widely different conclusions regarding the validity of the CDD, depending on whose data one chooses to use for the reciprocity relation.

Second, the Hubble diagram based on HIIGx and GEHR measurements may be used to determine the luminosity distance without the assumption of any particular cosmological model. This application is made possible through the use of Gaussian Processes to reconstruct the distance modulus as a function of redshift. Third, these two sets of data allow us to measure the CDD over a significantly larger redshift range than was possible with Type Ia SNe. Not only have we confirmed the CDD with a higher precision than before, but we have done so all the way out to $z \sim 2.5$.

Finally, we have demonstrated the practicality of this outcome by using it to test two competing cosmologies. We have shown that the measured CDD data favour the $R_h = ct$ universe over ΛCDM with a likelihood of $\sim 82.3\%$ versus only $\sim 17.7\%$, confirming the results of previously published model comparisons based on over 23 other kinds of data, which are summarized in Table 1 of Melia (2017b). In this regard, it is worth comparing this result with that of another recent application of the CDD by Hu & Wang (2018) to test the $R_h = ct$ and ΛCDM cosmologies. These workers based their analysis on an entirely different approach, with a significantly different conclusion.

How does one reconcile such different outcomes? In our case, the CDD was first confirmed independently of any cosmological model, and the results summarized in Equation (11) and fig. 4 are entirely consistent with $\eta(z) = 1$. In using the CDD to test our models, there was no need to include model fits to the compact quasar core and HIIGx GEHR data themselves, which would have obscured the true outcome based on the CDD itself. As such, there were no complications arising from the effects on $d_L(z)$ from the merger of sub-samples of sources with unknown intrinsic dispersions, or with non-uniform calibrations. Our comparison is clean and is directly based on the CDD itself.

In contrast, Hu & Wang (2018) did not use a cosmology-independent approach to examine the CDD, opting instead to base their analysis on older methods using galaxy clusters and Type Ia SNe. The outcome of their comparison is therefore heavily biased by the impact of fits to the cluster and SN data themselves, rather than being a true reflection of the CDD. Unfortunately, these fits—particularly to the Type Ia SN data—are heavily tainted by the many problems encountered with model comparisons based on such observations, as described in several published accounts (see, e.g., Kim 2011; Wei et al. 2015). Of particular concern with their work is the fact that their results are strongly dependent on the Hubble constant, which they demonstrated by comparing two values, though failing to optimize H_0 separately for each model. The most serious drawback with their approach, however, is simply ignoring the unknown systematic differences between sub-samples merged to produce the overall SN catalog. As demonstrated in Wei et al. (2015), one should ideally use a single SN sample, with a homogeneous calibration and systematics for all the data. But even then, that method of measuring the CDD is inferior to a true cosmology-independent approach, as we have in this paper, which produces an unbiased determination of $\eta(z)$ for model comparisons.

Finally, with an eye to possible future applications of this work, we recall several cautionary remarks we have made concerning the dependence of this work on possible unknown systematics in the quasar core and HII galaxy data. Given how well the test of the CDD has turned out with these sources, perhaps one should turn this procedure around and use the CDD to evaluate the internal self-consistency of the astrophysical models used for the radio emission and compact structure of the former, and the HII line emission and velocity dispersion in the latter. At the very least, an application of the CDD to such sources may delimit the extent to which any unaccounted for systematics and unknowns are impacting their observed spectra and luminosities.

In conclusion, the fact that the CDD is confirmed by the observations hardly surprises anyone. After all, many cosmological measurements tacitly assume its validity anyway. Nonetheless, the cosmology-independent approach we have used in this paper has provided a compelling demonstration that distance duality is indeed realized in nature.

ACKNOWLEDGMENTS

I am grateful to the anonymous referee for suggesting several improvements to this manuscript. I am also grateful to Amherst College for its support through a John Woodruff Simpson Lectureship, and to Purple Mountain Observatory in Nanjing, China, for its hospitality while part of this work was being carried out. This work was partially supported by grant 2012T1J0011 from The Chinese Academy of Sciences Visiting Professorships for Senior International Scientists, and grant GDJ20120491013 from the Chinese State Administration of Foreign Experts Affairs.

REFERENCES

Adler, S. L., 1971, AnPhy, 67, 599
Amanullah, R., Lidman, C., Rubin, D. et al. 2010, ApJ, 716, 712
Bassett, B. A. & Kunz, M., 2004a, ApJ, 607, 661
Bassett, B. A. & Kunz, M., 2004b, PRD, 69, 101305
Bélanger, G., Goldwurm, A., Goldoni, P., Paul, J., Terrier, R., Falanga, M. et al., 2004, ApJL, 601, L163
Bergeron, J., 1977, ApJ, 211, 62
Bernardis, F. D., Giusarma, E. & Melchiorri, A., 2006, IJMP-D, 15, 759
Blanchard, A., 2006, in: Current issues in Cosmology, eds. J.-C. Pecker and J. V. Narlikar, (Cambridge University Press, Cambridge U.K., p. 76
Blandford, R. D. & Königl, A., 1979, ApJ, 232, 34
Bordalo, V. & Telles, E., 2011, ApJ, 735, 52
Bosch, G., Terlevich, E. & Terlevich, R., 2002, MNRAS, 329, 481
Burrage, C., 2008, PRD, 77, 043009
Cao, S. et al., 2017, JCAP, 02, id. 012
Chan, C.-K., Liu, S., Fryer, C. L., Psaltis, D., Özel, F., Rockefeller, G. & Melia, F., 2009, ApJ, 701, 521
Chashchina, O. I. and Silagadze, Z. K., 2015, Universe, 1, 307
Chávez, R., Terlevich, E., Terlevich, R., Plionis, M., Bresolin, F., Basilakos, S. & Melnick, J., 2012, MNRAS Lett, 425, L56
Chávez, R., Terlevich, R., Terlevich, E., Bresolin, F., Melnick, J., Plionis, M. & Basilakos, S., 2014, MNRAS, 442, 3565
Chávez, R., Plionis, M., Basilakos, S., et al., 2016, MNRAS, 462, 2431
Chen, P., 1995, PRL, 74, 634
Crocker, R. M., Jones, D. I., Aharonian, F., Law, C. J., Melia, F. & Ott, J., 2011, MNRAS Letters, 411, L11
Deffayet, C. & Uzan, J.-P., 2000, PRD, 62, 063507
Ellis, G.F.R., 1971, in Proc. School "Enrico Fermi", Ed. R. K. Sachs, New York
Ellis, G.F.R., Poltis, R., Uzan, J.-P. & Weltman, A., 2013, PRD, 87, 103530
Etherington, I.M.H., 1933, Philos. Mag., 15, 761
Fatuzzo, M. & Melia, F., 2017, ApJ, 846, 129
Fuentes-Masip, O., Muñoz-Tuñón, C., Castañeda, H. O. & Tenorio-Tagle, G., 2000, AJ, 120, 752
Gurvits, L. I., 1994, ApJ, 425, 442
Gurvits, L. I., Kellermann, K. I. & Frey, S., 1999, A&A, 342, 378
Holanda, R.F.L., Lima, J. A. & Ribeiro, M. B., 2010, ApJL, 722, L233
Holanda, R.F.L., Lima, J. A. & Ribeiro, M. B., 2012, A&A, 538, A131
Hu, J. & Wang, F.-Y., 2018, MNRAS, in press (arXiv:1804.06606)
Jackson, J. C., 2004, JCAP, 11, id. 007
Jackson, J. C., 2008, MNRAS, 390, L1
Jackson, J. C. & Dodgson, M., 1997, MNRAS, 285, 806
Jackson, J. C. & Jannetta, A. L.,2006, JCAP, 11, 002
Kass, R. E. & Raftery, A. E., 1995, J. Amer. Stat. Ass., 90, 773
Kellermann K. I., 1993, Nature, 361, 134
Kim, A. G., 2011, PASP, 123, 230
Khedekar, S. & Chakraborti, S., 2011, PRL, 106, 221301
Khoury, J. & Weltman, A., 2004, PRL, 93, 171104
Kunth, D. & Östlin, G., 2000, A&ARv, 10, 1
LaViolette, P. A., 2012, Subquantum kinetics: The Alchemy of Creation, 4th ed. (Starlane Pub., Niskayana NY)
Leaf, K. & Melia, F., 2018a, MNRAS, 478, 5104
Leaf, K. & Melia, F., 2018b, MNRAS, 474, 4507
Li, Z., Wu, P. & Yu, H., 2011, ApJL, 729, L14
Liao, K., Avgoustidis, A. & Li, Z., 2015, PRD, 92, 123539
Liao, K., Li, Z., Cao, S., Biesiada, M., Zheng, X. & Zhu, Z.-H., 2016, ApJ, 822, 74
Liu, S. & Melia, F., 2001, ApJL, 561, L77
López-Corredoira, M., Melia, F., Lusso, E. and Risaliti, G., 2016, IJMP-D, 25, id. 1650060
Ma, C. & Corasaniti, P.-S., 2016, submitted (arXiv:1604.04631)
Mania, D. & Ratra, B., 2012, PhLB, 715, 9
Melia, F., Jokipii, J. R. & Narayanan, A., 1992, ApJL, 395, L87
Melia F., 2003, "The Edge of Infinity: Supermassive Black Holes in the Universe" (New York: Cambridge University Press), 158–171
Melia, F., 2007, MNRAS, 382, 1917
Melia, F., 2013a, A&A, 553, A76
Melia, F., 2013b, ApJ, 764, 72
Melia, F., 2014a, AJ, 147, 120
Melia, F., 2014b, JCAP, 01, 027
Melia, F., 2015, ASpSci 359, 34
Melia, F., 2016a, Front. Phys., 11, 119801
Melia, F., 2016b, Proc. R. Soc. A, 472, 20150765
Melia, F., 2017a, Front. Phys., 12, 129802
Melia, F., 2017b, MNRAS, 464, 1966
Melia, F., 2018a, EPL, 123, id. 39001
Melia, F., 2018b, EPJ-C, in press (arXiv:1809.02885)
Melia, F., 2018c, A&A, 615, A113
Melia, F. & Abdelqader, M., 2009, IJMP-D, 18, 1889
Melia, F. & Königl, A., 1989, ApJ, 340, 162
Melia, F. & López-Corredoira, M., 2017, IJMP-D, 26, id. 1750055
Melia, F. & López-Corredoira, M., 2018, A&A, 610, A87
Melia F. and Maier R. S., 2013, MNRAS, 432, 2669
Melia, F. and McClintock, T. M., 2015a, AJ, 150, id. 119
Melia, F. and McClintock, T. M., 2015b, Proc. R. Soc. A,
Melia, F. & Shevchuk, A., 2012, MNRAS, 419, 2579
Melia, F., Wei, J.-J. & Wu, X., 2015, AJ, 149, 2
Melia, F. & Yennapureddy, M. K., 2018, MNRAS, 480, 2144
Melnick, J., Moles, M., Terlevich, R. & Garcia-Pelayo, J.-M., 1987, MNRAS, 226, 849
Melnick, J., Terlevich, R. & Moles, M., 1988, MNRAS, 235, 297
Melnick, J., Terlevich, R. & Terlevich, E., 2000, MNRAS, 311, 629
Meng, X.-L., Zhang, T.-J., Zhan, H. & Wang, X., 2012, ApJ, 745, 98
Nair, R., Jhingan, S. & Jain, D., 2011, JCAP, 05, 023
Nayakshin, S. & Melia, F., 1998, ApJS, 114, 269
Planck Collaboration et al., 2016, A&A, 594, id A13
Plionis, M., Terlevich, R., Basilakos, S., Bresolin, F., Terlevich, E., Melnick, J. & Chavez, R., 2011, MNRAS, 416, 2981
Preston, R. A., 1985, AJ, 90, 1599
Raffelt, G. G., 1999, ARNPS, 49, 163
Santos, R. C. & Lima, J.A.S., 2008, PRD, 77, 083505
Schwarz, G. 1978, Ann. Statist., 6, 461
Searle, L. & Sargent, W.L.W., 1972, ApJ, 173, 25
Seikel, M., Clarkson, C. & Smith, M., 2012, JCAP, 06, 036S
Siegel, E. R., Guzmán, R., Gallego, J. P., Orduña-López, M. & Rodríguez-Hidalgo, P., 2005, MNRAS, 356, 1117
Sikivie, P., 1983, PRL, 51, 1415
Steinhardt, C. L., Capak, P., Masters, D. & Speagle, J. S., 2016, ApJ, 824, 1
Telles, E., 2003, ASPC, 297, 143
Terlevich, R. & Melnick, J., 1981, MNRAS, 195, 839
Terlevich, R., Terlevich, E., Melnick, J., Chávez, R., Plionis, M., Bresolin, F. & Basilakos, S., 2015, MNRAS, 451, 3001

Trap, G., Goldwurm, A., Dodds-Eden, K., Weiss, A., Terrier, R., Ponti, G. et al., 2011, A&A, 528, id. A140
Uzan, J.-P., Aghanim, N. & Mellier, Y., 2004, PRD, 70, 083533
Vauclair, S. C. et al., 2003, A&A, 412, L37
Vishwakarma, R. G., 2001, CQG, 18, 1159
Vishwakarma, R. G., 2013, Phys. Scr., 87, 055901
Wei, J.-J., Wu, X. and Melia, F., 2013, ApJ, 772, id. 43
Wei, J.-J., Wu, X. and Melia, F., 2014a, ApJ, 788, id. 190
Wei, J.-J., Wu, X., Melia, F., Wei, D.-M. and Feng, L.-L., 2014b, MNRAS, 439, 3329
Wei, J.-J., Wu, X., Melia, F., Wang, F.-Y. and Yu, H., 2015a, AJ, 150, id. 35
Wei, J.-J., Wu, X. and Melia, F., 2015b, AJ, 149, id. 165
Wei, J.-J., Wu, X., Melia, F. and Maier, R. S., 2015c, AJ, 149, id. 102
Wei, J.-J., Wu, X. and Melia, F., 2015d, MNRAS, 447, 479
Wei, J.-J., Wu, X.-F. & Melia, F., 2016, MNRAS, 463, 1144
Yang, X., Yu, H.-R., Zhang, Z.-S. & Zhang, T.-J., 2013, ApJL, 777, L24
Yennapureddy, M. K. & Melia, F., 2017, JCAP, 11, 029
Yennapureddy, M. K. & Melia, F., 2018a, EPJ-C, 78, 258
Yennapureddy, M. K. & Melia, F., 2018b, PDU, 20, 65
Yu, H. & Wang, F. Y., 2014, Eur. Phys. J. C, 74, 3090
Zeng, H., Melia, F. & Zhang, L., 2016, MNRAS, 462, 3094